

# Semantics-Guided Neural Networks for Efficient Skeleton-Based Human Action Recognition

Pengfei Zhang<sup>1\*</sup>   Cuiling Lan<sup>2†</sup>   Wenjun Zeng<sup>2</sup>   Jianru Xue<sup>1</sup>   Nanning Zheng<sup>1</sup>

<sup>1</sup> Institute of Artificial Intelligence and Robotics, Xian Jiaotong University   <sup>2</sup> Microsoft Research Asia  
zpengfei@stu.xjtu.edu.cn, {culan,wezeng}@microsoft.com, {jrxue,nnzheng}@mail.xjtu.edu.cn

## Abstract

*Skeleton-based human action recognition has attracted a lot of interests. Recently, there is a trend of using deep feed-forward neural networks to model the skeleton sequence which takes the 2D spatio-temporal map derived from the 3D coordinates of joints as input. Some semantics of the joints (frame index and joint type) are implicitly captured and exploited by large receptive fields of deep convolutions at the cost of high complexity. In this paper, we propose a simple yet effective semantics-guided neural network (SGN) for skeleton-based action recognition. We explicitly introduce the high level semantics of joints as part of the network input to enhance the feature representation capability. The model exploits the global and local information through two semantics-aware graph convolutional layers followed by a convolutional layer. We first leverage the semantics and dynamics (coordinate and velocity) of joints to learn a content adaptive graph for capturing the global spatio-temporal correlations of joints. Then a convolutional layer is used to further enhance the representation power of the features. With an order of magnitude smaller model size and higher speed than some previous works, SGN achieves the state-of-the-art performance on the NTU, SYSU, and N-UCLA datasets. Experimental results demonstrate the effectiveness of explicitly exploiting semantic information in reducing model complexity and improving the recognition accuracy.*

## 1. Introduction

Human action recognition has a wide range of application scenarios, such as video surveillance, human-computer interaction, and video retrieval [30, 44, 1]. In recent years, skeleton-based action recognition [50, 6, 31, 52] is attracting increasing interests. Skeleton is a type of well struc-

ture data with each joint of the human body identified by a joint type, a frame index, and a 3D coordinate position. There are several advantages of using skeleton for action recognition. First, skeleton is a high level representation of human body with the human pose and motion abstracted. Biologically, human is able to recognize the action category by observing only the motion of joints even without appearance information [14]. Second, the advance of cost effective depth cameras [54] and pose estimation technology [32, 3, 36] makes the access of skeleton much easier. Third, compared with RGB video, the skeleton representation is robust to variation of viewpoint and appearance. Forth, it is also computationally efficient because of low dimensional representation. Besides, skeleton-based action recognition is also complementary to the RGB-based action recognition [35]. In this work, we focus on skeleton-based action recognition.

For skeleton-based action recognition, deep learning is widely used to model the spatio-temporal evolution of the skeleton sequence [9, 41]. Various network structures have been exploited, such as Recurrent Neural Networks (RNNs) [6, 55, 31, 34, 51, 33], Convolutional Neural Networks (CNNs) [15, 52, 25, 45], and Graph Convolutional Networks (GCNs) [48, 33, 37]. In the early years, RNN/LSTM was the favored network to be used to exploit the short and long term temporal dynamics. Recently, there is a trend of using feedforward (*i.e.*, non-recurrent) convolutional neural networks for modeling sequences in speech, language [29, 8, 47, 42], and skeleton [15, 52, 25, 45] due to their superior performance. Most of the skeleton-based works organize the coordinates of joints to a 2D map and resize the map to a size (*e.g.*  $224 \times 224$ ) suitable for the input of a specific network (*e.g.* ResNet[10]). Its rows/columns correspond to the different types of joints/frames indexes. In these methods [15, 52, 25, 45], long-term dependencies and semantic information are expected to be captured by the large receptive fields of deep networks. This appears to be brutal and typically results in high model complexity.

Intuitively, semantic information, *i.e.* the frame index and joint type, is very important for action recognition.

\*This work was done when P. Zhang was an intern at Microsoft Research Asia.

†Corresponding author.

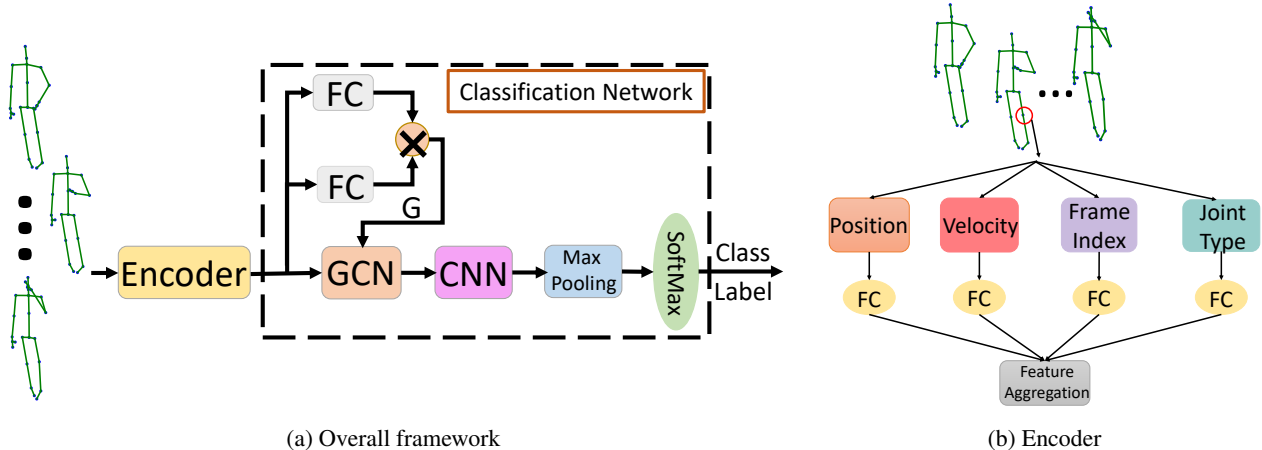


Figure 1: Flowchart of our proposed end-to-end Semantics-Guided Neural Network (SGN). (a) Our light weight network consists of an encoder for encoding the semantics and dynamics of each joint, the learned content-adaptive adjacency matrix  $G$  for spatio-temporal graph, two semantics-aware graph convolutional layers, one semantics-aware convolutional layer, and one SoftMax layer, for efficient classification. (b) Illustration of our proposed encoder. Given a joint of a skeleton sequence (marked as red circle), two pieces of dynamic information, *i.e.* position and velocity, and two pieces of semantic information, *i.e.*, frame index and joint type, are aggregated together to enhance the representation power of one joint.

Semantics together with coordinates reveal the spatial and temporal configuration/structure of human body joints. As we know, two joints of the same coordinates but different semantics would deliver very different information. For example, for a joint above the head, if this joint is a hand joint, the action is likely to be “raising hand”; if it is a foot joint, the action may be “kicking a leg”. However, most approaches [9, 41] overlook the importance of the semantic information and under-explore it.

To address the above mentioned limitations of current approaches, we propose a semantics-guided neural network (SGN) to explicitly exploit the semantics for highly efficient skeleton-based action recognition. Fig. 1a shows the overall framework. First, we explicitly include the semantics (frame index and joint type) together with the dynamics (position and velocity) in the input representation for each joint and encode them to an embedding vector. The architecture of the encoder is illustrated in Fig. 1b. Then, two semantics-aware graph convolutional layers and one semantics-aware convolutional layer are used to explore the global and local information. Note that the “semantics-aware” here denotes that the joint semantics is used as part of the input of graph convolutional and convolutional layers to make it easier for the models to leverage the semantics in feature learning. Global correlations of joints are explored by the semantics-aware graph convolutional layers while the discriminating feature learning is enhanced by the semantics-aware convolutional layer. Thanks to the efficient exploration of semantic information and global information, our proposed SGN achieves the state-of-the-art performance with very

few convolutional layers.

In summary, our contributions are two-fold:

- We propose to explicitly explore the joint semantics (frame index and joint type) for efficient skeleton-based action recognition. Previous works overlook the importance of semantics and rely on deep networks with high complexity for action recognition.
- We propose a semantics-guided neural network (SGN) to exploit the global and local correlations of joints for skeleton-based action recognition. With the guidance of the semantics, SGN is efficient both in learning spatio-temporal graph for capturing the global correlations and in enhancing the feature representation learning through local convolution.

Our proposed end-to-end SGN is simple yet effective. Compared to one latest representative work [33], SGN achieves a speedup in training and inferring by an order of magnitude, with only about ten percent of number of parameters.

## 2. Related Work

Skeleton-based action recognition has attracted increasing attentions recently. Recent works using neural networks [9] have significantly outperformed traditional approaches that use hand-crafted features [9, 46, 39, 49, 7].

**Recurrent Neural Network based.** Recurrent neural networks, such as LSTM [11] and GRU [4], are often used to model the temporal dynamics of skeleton sequence

[6, 31, 55, 51, 53]. The 3D coordinates of all joints in a frame are concatenated in some order to be the input vector of a time slot. They do not explicitly tell the networks which dimensions belongs to which joint. Some other RNN-based works tend to design special structures in RNN to make it aware of the spatial structural information. Shahroudy *et al.* [31] divide the cell of LSTM [11] into five sub cells corresponding to five body parts, *i.e.*, torso, two arms, and two legs, respectively. Liu *et al.* [22] propose a spatial-temporal LSTM model to exploit the contextual dependency of joints in both the temporal and spatial domain. At each step, they feed different types of joints. To some extent, they distinguish the different joints.

**Convolutional Neural Network based.** In recent years, in the field of speech, language sequence modeling, feed-forward convolutional neural networks demonstrate their superiority in both accuracy and parallelism [29, 8, 47, 42, 38]. The same is true for skeleton-based action recognition [5, 19, 15]. These CNN-based works transform the skeleton sequence to skeleton map of some target size and then use a popular network, such as ResNet [10], to explore the spatial and temporal dynamics. Some works transform a skeleton sequence to an image by treating the joint coordinate (x,y,z) as the R, G, B channels of a pixel [5, 19]. Ke *et al.* [15] transform the original skeleton sequence to four 2D arrays, which are represented by the relative position between four selected reference joints (*i.e.*, the left/right shoulder, the left/right hip) and other joints. Skeleton is well structured data with explicit high level semantics, *i.e.*, frame index and joint type. However, the kernels/filters of CNNs are translation invariant [26] and thus cannot directly perceive the semantics from such input skeleton maps. The CNNs are expected to be aware of such semantics through large receptive fields of deep networks, which is not very efficient.

**Graph Convolutional Network based.** Graph convolutional networks [17], which have been proven to be effective for processing structured data, have also been used to model the structured skeleton data. Yan *et al.* [48] propose a spatial and temporal graph convolutional network. They treat each joint as a node of the graph. The presence of edge denoting the joint relationship is pre-defined by human based on prior knowledge. Tang *et al.* [37] define the edges for both physically disconnected joint pairs and physically connected joint pairs for better constructing the graph. Si *et al.* [33] learn the graph edge of five human body parts within each frame using a data-driven method instead of human definition. However, the important semantics is not utilized for learning the graph edge. It is difficult to use joint coordinates alone to identify the joint type and learn the graph edge.

In summary, previous works for skeleton-based action recognition overlook the importance of explicitly exploiting

the semantics, *e.g.*, frame index and joint type. In this work, we investigate the explicit exploitation of semantics leveraging both GCN and CNN and design a simple yet effective neural network for skeleton-based action recognition.

### 3. Semantics-Guided Neural Networks

For a skeleton sequence, we identify a joint by its semantics (frame index and joint type) and represent it together with its dynamics (position/3D coordinate and velocity). Without semantics, the skeleton data will lose the important spatio-temporal structure. Previous CNN-based works [15, 5], however, typically overlook the semantics by implicitly hiding them in the 2D skeleton map (*e.g.* with rows corresponding to the different types of joints and columns corresponding to the frame indexes).

We propose a semantics-guided neural network (SGN) for skeleton-based action recognition and show the overall end-to-end framework in Fig. 1a. For a skeleton sequence, a joint encoder encodes the semantics and dynamics of each joint into four embedding vectors as illustrated in Fig. 1b. For a sequence, with each joint as a node, a spatio-temporal graph is adaptively constructed based on the semantics and dynamics. Then two graph convolutional layers are used to explore the global correlations, and one convolutional layer is used to explore the local correlations and enrich the representational power of features. Afterward, a max pooling layer and a softmax layer are used to generate the class label with standard cross entropy loss. More details about each component are described in the following subsections.

Specifically, for a skeleton sequence, we denote all the joints as a set  $\mathcal{S} = \{ X_t^j \mid t = 1, 2, \dots, T; j = 1, 2, \dots, J \}$ , where  $X_t^j$  denotes the joint of type  $j$  at time  $t$ .  $T$  denotes the number of frames of the skeleton sequence and  $J$  denotes the total number of joints of a human body in a frame.

#### 3.1. Encoder

For a given joint  $X_t^j$  of type  $j$  at time  $t$ , it can be identified by its dynamics and semantics. Dynamics is defined as its position  $\mathbf{p}_{t,j} = (x_{t,j}, y_{t,j}, z_{t,j})^T$  in the 3D coordinate system, and velocity  $\mathbf{v}_{t,j} = \mathbf{p}_{t,j} - \mathbf{p}_{t-1,j}$ . Semantics means the frame index  $t$  and joint type  $j$ . Both frame index and joint type are represented by a one hot vector as  $\mathbf{f}_t \in \mathbb{R}^{J^1}$ ,  $\mathbf{j}_j \in \mathbb{R}^T$ , respectively. As illustrated in Fig. 1b, the encoder respectively embeds the four pieces of information to a high dimensional space and aggregate them by concatenation. Because the four pieces of raw representations are not in the same domain, separate embedding in the same manner is performed with unshared parameters.

Take the embedding of position as an example. We encode the position using two fully connected (FC) layers as

<sup>1</sup>For the one hot vector  $\mathbf{f}_t$  of frame  $t$ , all the elements are zero except the  $t^{th}$  is 1.

$$\widetilde{\mathbf{p}}_{t,j} = \sigma(W_1(\sigma(W_2\mathbf{p}_{t,j}))), \quad (1)$$

where  $W_1$  and  $W_2$  are two matrices, the biases are omitted to simplify the notation,  $\sigma$  denotes the ReLU activation function [28].

Similarly, for the given joint  $X_t^j$ , using respective FC layers, we obtain the embedding for velocity, frame index, and joint type respectively as  $\widetilde{\mathbf{v}}_{t,j}$ ,  $\widetilde{\mathbf{f}}_t$ ,  $\widetilde{\mathbf{j}}_j$ .

The four pieces of information describe a joint from different aspects. We aggregate them together through concatenation to fully represent one joint as  $\mathbf{z}_{t,j} = [\widetilde{\mathbf{p}}_{t,j}, \widetilde{\mathbf{v}}_{t,j}, \widetilde{\mathbf{f}}_t, \widetilde{\mathbf{j}}_j] \in \mathbb{R}^d$ , where  $d$  is the dimension of the joint representation.

### 3.2. Classification Network

The classification network consists of two sub modules to exploit the correlations of joints globally and locally. Two semantics-aware graph convolutional layers are first used to capture the long range correlations of joints. A semantics-aware convolutional layer is then used to further enhance the representation capability of the learned features. Note that we embed the joint semantics as part of the input of the classification network through an encoder. Thus it is natural to apply the graph convolutional layers to exploit the explicit semantics (together with dynamics) by building the content adaptive connections within the graph to exploit the structural information of skeleton data. We use ‘‘semantics-aware’’ here to emphasize that the inputs of the networks contain semantics which helps improve the efficiency of both modules. In the following, we introduce the two sub modules in detail.

**Semantics-aware graph convolution.** To model the structural skeleton data for action recognition, some GCN-based works take the joints as nodes and pre-define the graph connection (edge) based on prior knowledge [48]. For example, the physically connected joints are defined as connected and others are defined unconnected. Human defined connection is not optimal. Besides, for different actions, the correlations between two joints are different. Meanwhile, even in one sequence, the correlation between two nodes varies as time evolves. Thus, we build adaptive graph where the edges between different nodes depend on the content instead of human prior. We propose to use two semantics-aware graph convolutional layers to globally exploit the structural information.

To learn the graph connections, besides the joint dynamics, *i.e.*, position and velocity, the semantics, *i.e.*, frame index and joint type, are also very important. First, as we know, the human defined graph connections are pre-defined based on only the semantics. This indicates the semantics has already provided useful information. Second, it does not make sense to only rely on the dynamics (position, velocity) to determine the graph connection. As is known, the

dynamics of different joint pairs may be the same. However, the connected edge weights should be different since the relationships are different for pairs of different semantics. We thus propose to use both dynamics and semantics to learn the graph.

Given a skeleton sequence with  $T$  frames and  $J$  joints in each frame, we build a graph of  $N = T \times J$  nodes. We denote the joint of frame  $t$  and of joint type  $j$ , *i.e.*,  $\mathbf{z}_{t,j}$ , as the  $k^{th}$  node  $\mathbf{z}_k$  where  $k = J(t - 1) + j$ . We denote the input as  $Z = (\mathbf{z}_1, \dots, \mathbf{z}_N)^T \in \mathbb{R}^{N \times d}$ . Similar to [43, 42], the edge weight from the  $i^{th}$  to the  $j^{th}$  joint is represented by their similarity/affinity in the transformed space as

$$F(\mathbf{z}_i, \mathbf{z}_j) = \phi_1(\mathbf{z}_i)^T \phi_2(\mathbf{z}_j), \quad (2)$$

where  $\phi_1$  and  $\phi_2$  denote two transformation functions with each constructed by an FC layer, *i.e.*,  $\phi_1(\mathbf{z}_i) = W_3\mathbf{z}_i + \mathbf{b}_3$  and  $\phi_2(\mathbf{z}_j) = W_4\mathbf{z}_j + \mathbf{b}_4$ .

By computing the affinities of all the joint pairs based on (2), we can obtain the adjacency matrix. Normalization using SoftMax as [38, 42] is performed on each row so that the sum of all the edge values connected to one node is 1. We denote the normalized adjacency matrix by  $G$  for spatio-temporal graph. A residual graph convolution layer is used to realize global message passing among nodes as

$$\begin{aligned} Y &= GZW, \\ Z' &= W_y Y + W_z Z, \end{aligned} \quad (3)$$

where  $W$  aims to further embed  $Z$ ;  $W_y$  and  $W_z$  are transformation matrices that facilitate the residual fusion at the same domain.  $Z'$  is the output.  $G$  is the adjacency matrix with  $N \times N$  dimensions. Note that one can stack multiple residual graph convolution layers to enable further message passing among nodes with the same adjacency matrix  $G$ .

**Semantics-aware convolution.** GCN facilitates the exploration of global correlations of joints. For each node, it is equivalent that this node has *one* global large kernel that covers all the nodes on exploring one pattern to mine global correlations of other joints. In comparison, a CNN layer has smaller kernels with each kernel focusing on exploring some pattern to mine the local correlations of joints. The diversity of CNN kernels makes it powerful on learning features through mining patterns. To enhance the representation of learned features, we add a standard convolutional layer after the GCN. The output of the semantics-aware graph convolutional layers that corresponds to  $N = T \times J$  joints is rearranged to be a  $T \times J$  feature map to be used as the input of this CNN layer. Each position of this feature map contains both the semantics and dynamics and this facilitates the convolutional layer to learn discriminative features.

## 4. Experiments

In the following, we demonstrate the effectiveness of the proposed semantic-guided neural networks for skeleton-based action recognition. We first describe the datasets and the implementation details in Subsection 4.1. In Subsection 4.2, we perform ablation studies to analyze how our model works. In Subsection 4.3, we compare our SGN with the state-of-the-art approaches on three benchmark datasets. Subsection 4.4 discuss the complexity of SGN in comparison with other approaches.

### 4.1. Datasets and Implementation Details

#### 4.1.1 Datasets

**NTU RGB+D Dataset (NTU) [31].** This dataset is collected by Kinect camera and is currently the largest RGB+D dataset for 3D action recognition with 56880 skeleton sequences. It contains 60 action classes performed by 40 different subjects. Each human skeleton is represented by 25 joints with 3D coordinates. For Cross Subject (CS) setting [31], half of the 40 subjects are used for training and the rest for testing. For Cross-View (CV) setting [31], the sequences captured by two of the three cameras are used for training and the other camera is used for testing. In addition, following [31], we randomly select 10% of the training sequences for validation for both the CS and CV settings.

**SYSU 3D Human-Object Interaction Dataset (SYSU) [12].** This dataset is collected by Kinect camera. It contains 480 skeleton sequences of 12 actions performed by 40 different subjects. Each human skeleton has 20 joints. We use the same evaluation protocols as [12]. For the Cross Subject (CS) setting, half of the subjects are used for training and the rest for testing. For the Same Subject (SS) setting, half of the samples of each activity are used for training and the rest for testing. We use the 30-fold cross-validation and show the mean accuracy for each setting [12].

**Northwestern-UCLA Dataset (N-UCLA) [40].** This dataset consists of 1494 skeleton sequences. It includes 10 actions performed by 10 different subjects. Each human skeleton is represented by 20 joints. We adopt the same evaluation protocol as [40], *i.e.*, the samples captured by the first two cameras are used for training, and those captured by the third cameras for testing.

#### 4.1.2 Implementation Details

**Network setting.** For the encoder, the neuron number is set to 64 for each FC layer. Note that the weights of FC layers are not shared for the four types of input. For the transformation function in (2), the neuron number of the FC layer is set to 256. For the CNN layer following GCN, we set the kernel number to 512 with kernel size of  $3 \times$

3. After each GCN or CNN layer, batch normalization [13] and ReLU nonlinear activation function are used.

**Optimization setting.** All experiments are conducted on the Pytorch platform. We use the Adam [16] optimizer with the initial learning rate of 0.001. The learning rate is divided by 10 when the validation accuracy plateaus. We use a weight decay of 0.0001. The batch sizes of NTU, SYSU, and N-UCLA datasets are set to 64, 16 and 16, respectively.

**Data processing.** Similar to [51], sequence level translation based on the first frame is performed to be invariant to the initial position. If one frame contains two human skeletons, we rebuild the frame to two frames by making each frame contain one human skeleton. During training, according to [22], we segment the entire skeleton sequence into 20 clips equally, and randomly select one frame from each clip to make a new sequence which consists of 20 frames. During testing, similar to [2], we randomly create 5 new sequences in the similar manner and the mean score is used to predict the class.

We perform data argumentation by randomly rotating the skeletons by some degrees to be robust to the view variation during training. For the NTU dataset (CS setting), SYSU, and N-UCLA datasets, we randomly select one degree between  $[-17^\circ, 17^\circ]$  for one sequence. Considering that the view variation is large for the CV setting of NTU dataset, we randomly select one degree between  $[-30^\circ, 30^\circ]$  for one sequence.

### 4.2. Ablation Study

In Subsection 4.2.1, we evaluate the effectiveness of explicitly exploiting semantics. In Subsection 4.2.2, we make comparison of the effectiveness of semantic-aware GCN versus stacking multiple CNN layers for exploring global correlations. We discuss the influence of the depth of GCN and CNN in Subsection 4.2.3. To better understand the learned spatio-temporal graph, we perform some visualizations in Subsection 4.2.4.

#### 4.2.1 Effectiveness of Exploiting Semantics

Semantics contains the important structural information of a skeleton sequence and is important for skeleton-based action recognition. To demonstrate the effectiveness of exploiting semantics, by referencing our framework (see Fig. 1a), we build five neural networks and perform various experiments for the NTU CS setting. In the following, *Sem.* denotes semantics, *G* denotes the learning of spatio-temporal graph, *P* denotes the graph convolutional operations which enable the message passing.

**CNN w/o Sem.** or **CNN w Sem.** contains an encoder and one CNN layer. They are both built by removing the GCN layer in our scheme (see Fig. 1a). The semantics is not included in the encoder for the *CNN w/o Sem.* model,

Table 1: Effectiveness of exploiting semantics on the CNN and GCN&CNN, on the NTU CS setting, in accuracy (%).

Method	Acc.
CNN w/o Sem.	82.2
CNN w Sem.	84.1
GCN(G w/o Sem. & P w/o Sem.)&CNN	82.9
GCN(G w Sem. & P w/o Sem.)&CNN	83.6
GCN(G w Sem. & P w Sem.)&CNN	85.8

and is included for the *CNN w Sem.* model.

**GCN(G w/o Sem. & P w/o Sem.)&CNN** contains an encoder, one GCN layer, and one CNN layer. The encoder only encodes the dynamics. The semantic information is not used for learning spatio-temporal graph ( $G$ ) and does not take part in the graph convolutional operations for message passing ( $P$ ).

**GCN(G w Sem. & P w/o Sem.)&CNN** contains an encoder, one GCN layer, and one CNN layer. The encoder encodes both semantics and dynamics. Both semantics and dynamics are used for learning the graph  $G$  but the graph convolutional operations are only performed on the dynamics.

**GCN(G w Sem. & P w Sem.)&CNN** contains an encoder, one GCN layer, and one CNN layer. Both semantics and dynamics are used for learning the graph  $G$  and take part in the graph convolutional operations.

From the results in Table 1, we have the following observations. **1)** “CNN w Sem.” outperforms “CNN w/o Sem.” by 1.9%. This indicates that the semantics together with the dynamics facilitate learning better feature representations for action recognition. **2)** For the learning of spatio-temporal graph of skeleton sequence, with the semantics considered, “GCN(G w Sem. & P w/o Sem.)&CNN” outperforms “GCN(G w/o Sem. & P w/o Sem.)&CNN” by 0.7%. If the model does not know the semantics of the joints, it then cannot distinguish the joints with the same coordinates even though their semantics are rather different. **3)** When the semantics is used for the learning of graph and the graph convolutional operations, a superior performance is achieved, which outperforms “GCN(G w/o Sem. & P w/o Sem.)&CNN” by 2.9%. In summary, the semantics helps for both the convolution and graph convolution.

Hereafter, we will take semantics, *i.e.*, frame index and joint type, as parts of the input in the encoder by default within our network design to simplify notation, unless explicitly denoted with “w/o Sem.”.

#### 4.2.2 Efficiency of GCN vs. Multilayer CNN

Different from some previous works that exploit the global correlations of joints and implicit semantics by deep net-

Table 2: Comparison of GCN and multilayer CNN in terms of accuracy (%) and number of parameters.

Model	# Params	Acc.
CNN(1-layer)	1.2M	84.1
CNN(2-layer)	1.8M	84.6
CNN(3-layer)	4.2M	85.0
CNN(4-layer)	6.5M	85.3
CNN(5-layer)	8.9M	85.5
CNN(1-layer) w/o Sem.	0.6	82.2
CNN(2-layer) w/o Sem.	1.5M	84.1
CNN(3-layer) w/o Sem.	3.9M	84.8
CNN(4-layer) w/o Sem.	6.2M	84.9
CNN(5-layer) w/o Sem.	8.6M	85.0
GCN(1-layer)&CNN(1-layer)	1.6M	85.8

works, we use a shallow network with the explicit semantics as input, which consists of one GCN layer and one CNN layer. We compare our shallow network with the deep networks and study the influence of explicit semantics on deep networks within our network design in Table 2.

**CNN( $n$ -layer) or CNN( $n$ -layer) w/o Sem.** contains an encoder and  $n$  CNN layers. The semantics is included in *CNN( $n$ -layer)* model, and is not included in *CNN( $n$ -layer) w/o Sem.* model. For *CNN(1-layer)* or *CNN(1-layer) w/o Sem.*, we use 512 kernels. For *CNN(2-layer)* and *CNN(2-layer) w/o Sem.*, we use 256 and 512 kernels for each model. For the model with more than 2 CNN layers, we just simply stacking additional CNN layers with 512 kernels.

**GCN(1-layer)&CNN(1-layer)** contains an encoder, one GCN layer with 256 hidden neurons, and one CNN layer with 512 kernels.

Note that the kernel size is  $3 \times 3$  for all CNN layers.

From Table 2, we observe that the performance improves as the network goes deeper for both the networks with semantics and without semantics. However, with the same number of CNN layers, the models with semantics are better than those without semantics. Particularly, with fewer CNN layers, the performance of “CNN(3-layer)” is the same as that of “CNN(5-layer) w/o Sem.”. It demonstrates that using the explicit semantics as input of the models is more effective. Explicit semantics reduces the need for exploring the implicit semantics by deeper networks.

We also observe that, with similar number of parameters, “GCN(1-layer)&CNN(1-layer)” outperforms “CNN(2-layer)” by 1.2%. With much smaller number of parameters, “GCN(1-layer)&CNN(1-layer)” outperforms “CNN(5-layer)” by 0.3%. GCN is able to capture the global correlations of joints through the adaptive spatio-temporal graph and is more effective than deep networks with respect to exploration of global correlations. Though the deep net-

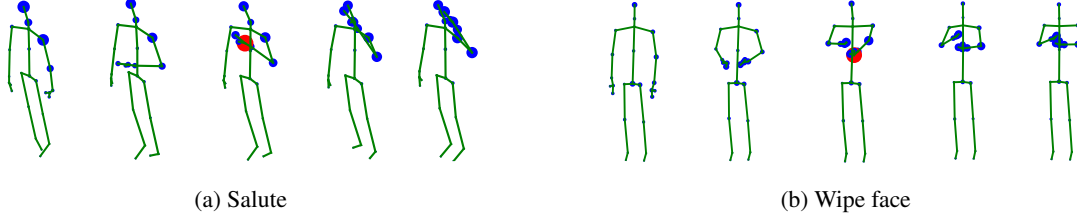


Figure 2: Visualization of our learned spatio-temporal graph. The query joint is marked as red solid circle. The blue solid circle denotes the correlations between the query joint and other joints of adjacent frames. The larger the correlation, the larger the solid circle size. (a) and (b) show the examples of actions *salute* and *wipe face*, respectively. For each action, we select 5 frames in time order to represent the whole action. The query joints are at the middle of the action.

Table 3: Comparison between GCNs and CNNs with different depths for the NTU CS setting in terms of accuracy (%) and number of parameters.

Model	# Params	Acc.
GCN(1-layer)&CNN(0-layer)	0.4M	82.0
GCN(0-layer)&CNN(1-layer)	1.2M	84.1
GCN(1-layer)&CNN(1-layer)	1.6M	85.8
GCN(2-layer)&CNN(1-layer)	1.8M	86.6
GCN(3-layer)&CNN(1-layer)	2.0M	86.7
GCN(2-layer)&CNN(2-layer)	4.1M	86.4

work can capture global correlations through large receptive field to some extent, the effective receptive field is limited [27]. In contrast, the effective receptive field of GCN is the whole skeleton sequence.

### 4.2.3 Depth of GCN and CNN

We show the influence of depth of GCN and CNN in Table 3. “GCN(n-layer)&CNN(n-layer)” contains an encoder, n CNN layers with 512 kernels, and n GCN layers with 256 hidden neurons.

GCN and CNN are not effective enough alone. “GCN(1-layer)&CNN(1-layer)” achieves a high performance of 85.8% after combining two models together. CNN further enhances the representation capability of the learned global features by GCN.

The accuracy keeps increasing when stacking more GCN layers. However, the gain is minor when using three GCN layers in comparison with two GCN layers. We use two GCN layers in our final scheme.

Stacking two CNN layers decreases the performance in comparison with one CNN layer when using two GCN layers. Therefore, we use one CNN layer in our final scheme.

### 4.2.4 Visualization of Spatio-Temporal Graph

Fig. 2a shows, for an example of the action of *salute*, the correlations between the left hand joint of the 14<sup>th</sup> frame and all other joints. The figures show the 1<sup>st</sup>, 13<sup>th</sup>, 14<sup>th</sup>, 15<sup>th</sup>, and 17<sup>th</sup> frames from left to right. The correlation between the query joint (left hand of 14<sup>th</sup>) and left thumb of 1<sup>st</sup> frame is weak, but the correlation becomes stronger as the action develops. The correlations of joints in the 17<sup>th</sup> frame which are important for *salute*, e.g., left thumb, left elbow, and head, are strong.

Fig. 2b shows, for an example of the action of *wipe face*, the correlations between the query joint left hand joint of the 8<sup>th</sup> frame and all other joints. The figures show the 1<sup>st</sup>, 5<sup>th</sup>, 8<sup>th</sup>, 15<sup>th</sup>, and 19<sup>th</sup> frames from left to right. Different from the action *salute*, *wipe face* is completed with two hands together. Our spatio-temporal graph shows the strong correlations between right hands of 8<sup>th</sup>, 15<sup>th</sup>, and 19<sup>th</sup> frames and the query joint.

Different from the pre-defined graph which is based on the human prior knowledge, the correlations of joints of learned spatio-temporal graph differ for different actions and different frames, which is consistent with human intuition.

### 4.3. Comparison with State-of-the-Art

We compare our proposed SGN with other state-of-the-art methods on the NTU, SYSU, and N-UCLA datasets in Table 4, Table 5, and Table 6, respectively. The SGN consists of an encoder, two GCN layers, and one CNN layer. SGN w/o Sem. is similar to SGN, but does not include semantics in the encoder.

As shown in Table 4, SGN achieves the best performance for both the CS and CV settings of NTU dataset. [53] and [15] are two representative methods for RNN-based and CNN-based methods, SGN outperforms them by 5.9% and 7.0% for the NTU CS setting, respectively. To better explore the structural information of skeleton, some methods [48, 33] mixed CNN and GCN, or LSTM and GCN together. Our proposed SGN is still superior to [48] and [33] by 5.1% and 1.8% for the NTU CS setting because of the semantics and our content-based spatio-temporal graph.

Table 4: Performance comparisons on the NTU dataset with the CS and CV settings in terms of accuracy (%).

Method	Year	CS	CV
HBRNN-L [6]	2015	59.1	64.0
Part-aware LSTM [31]	2016	62.9	70.3
ST-LSTM + Trust Gate [22]	2016	69.2	77.7
STA-LSTM [34]	2017	73.4	81.2
GCA-LSTM [24]	2017	74.4	82.8
URNN-2L-T [20]	2017	74.6	83.2
Clips+CNN+MTLN [15]	2017	79.6	84.8
VA-LSTM [51]	2017	79.4	87.6
EiAtt-GRU[53]	2018	80.7	88.4
ST-GCN [48]	2018	81.5	88.3
DPRL+GCNN [37]	2018	83.5	89.8
SR-TSL [33]	2018	84.8	92.4
SGN w/o Sem.	-	84.9	90.5
SGN	-	<b>86.6</b>	<b>93.4</b>

Table 5: Performance comparisons on the SYSU dataset in terms of accuracy (%).

Method	Year	CS	SS
VA-LSTM [51]	2017	77.5	76.9
ST-LSTM [21]	2018	76.5	-
DPRL+GCNN [37]	2018	76.9	-
GCA-LSTM [23]	2018	78.6	-
SR-TSL [33]	2018	81.9	80.7
EiAtt-GRU [53]	2018	85.7	85.7
SGN w/o Sem.	-	84.4	83.1
SGN	-	<b>86.9</b>	<b>86.5</b>

In addition, our proposed SGN outperforms the best state-of-the-art method [33] by 1.8% and 1.0% for CS and CV settings, respectively.

As shown in Table 5 and Table 6, our proposed SGN achieves the best accuracy for the SYSU and N-UCLA datasets. It should be noted that we used the pre-trained model on the NTU dataset to initialize the model for SYSU and N-UCLA datasets as was done in [53].

#### 4.4. Complexity of SGN

We discuss the complexity of SGN by comparing our model with three state-of-the-art methods for skeleton-based action recognition in Table 7. VA-LSTM only includes LSTM layers, ST-GCN includes both CNN and GCN layers, and SR-TSL includes both LSTM and GCN layers.

As shown in Table 7, the number of parameters of VA-LSTM is the least, but the accuracy and inference speed are the poorest. SR-TSL achieves good accuracy, but the

Table 6: Performance comparisons on the N-UCLA dataset in terms of accuracy (%).

Method	Year	Acc.
HBRNN-L [6]	2015	78.5
Visualization CNN[25]	2017	86.1
Ensemble TS-LSTM [18]	2017	89.2
EleAtt-GRU [53]	2018	90.7
SGN w/o Sem.	-	91.2
SGN	-	<b>92.5</b>

Table 7: Comparison with other state-of-the-art methods for the NTU CS setting in terms of accuracy (%), number of parameters, and inference speed. Speed denotes sequences per second. When inferring, we set the batch size to 1.

Scheme	Year	# Params	Acc.	Speed
VA-LSTM [51]	2017	0.5	79.4	7.9 <sup>1</sup>
ST-GCN [48]	2018	3.1	81.5	42.9 <sup>2</sup>
SR-TSL [33]	2018	19.1	84.8	14.0 <sup>1</sup>
SGN	-	<b>1.8</b>	<b>86.6</b>	<b>188.0</b>

<sup>1</sup> The results are obtained by consulting the authors.

<sup>2</sup> The results are obtained by the released code.

number of parameters is so large, and the inference speed is slow. The number of parameters of ST-GCN is smaller, but this method is not efficient in both training and testing. With one P100 GPU card, it takes about 20 minutes per epoch during training (ours is 0.7 minute per epoch) and the inference speed is slow too because of its deep network structure. Our model achieves the best performance, with small model size and high inference speed.

## 5. Conclusion

In this work, we propose a simple yet effective end-to-end semantics-guided neural network. We explicitly introduce the high level semantics, *i.e.*, frame index and joint type, as part of the network input. To model the correlations of joints, we propose a semantics-aware graph convolution subnetwork with content adaptive spatio-temporal graph for capturing the long-range correlations of joints within a skeleton sequence, and a semantics-aware CNN subnetwork for capturing the short-range correlations of joint features. The semantics helps improve the capability of graph convolution and CNN. Experimental results demonstrate that our proposed model is much more efficient than simply stacking multiple CNN layers. With an order of magnitude smaller model size than some previous works, our proposed model achieves the state-of-the-art results on three benchmark datasets with high inference speed.



## References

- [1] J. K. Aggarwal and M. S. Ryoo. Human activity analysis: A review. *ACM Computing Surveys*, 2011.
- [2] F. Baradel, C. Wolf, J. Mille, and G. W. Taylor. Glimpse clouds: Human activity recognition from unstructured feature points. In *CVPR*, 2018.
- [3] Z. Cao, T. Simon, S.-E. Wei, and Y. Sheikh. Realtime multi-person 2d pose estimation using part affinity fields. In *CVPR*, 2017.
- [4] K. Cho, B. Van Merriënboer, C. Gulcehre, D. Bahdanau, F. Bougares, H. Schwenk, and Y. Bengio. Learning phrase representations using rnn encoder-decoder for statistical machine translation. *arXiv*, 2014.
- [5] Y. Du, Y. Fu, and L. Wang. Skeleton based action recognition with convolutional neural network. In *ACPR*, 2015.
- [6] Y. Du, W. Wang, and L. Wang. Hierarchical recurrent neural network for skeleton based action recognition. In *CVPR*, 2015.
- [7] G. Garcia-Hernando and T.-K. Kim. Transition forests: Learning discriminative temporal transitions for action recognition and detection. In *CVPR*, 2017.
- [8] J. Gehring, M. Auli, D. Grangier, D. Yarats, and Y. N. Dauphin. Convolutional sequence to sequence learning. In *ICML*, 2017.
- [9] F. Han, B. Reily, W. Hoff, and H. Zhang. Space-time representation of people based on 3d skeletal data: A review. *CVIU*, 2017.
- [10] K. He, X. Zhang, S. Ren, and J. Sun. Deep residual learning for image recognition. In *CVPR*, 2016.
- [11] S. Hochreiter and J. Schmidhuber. Long short-term memory. *Neural computation*, 1997.
- [12] J.-F. Hu, W.-S. Zheng, J. Lai, and J. Zhang. Jointly learning heterogeneous features for rgb-d activity recognition. In *CVPR*, 2015.
- [13] S. Ioffe and C. Szegedy. Batch normalization: Accelerating deep network training by reducing internal covariate shift. *arXiv*, 2015.
- [14] G. Johansson. Visual perception of biological motion and a model for its analysis. *Perception & psychophysics*, 1973.
- [15] Q. Ke, M. Bennamoun, S. An, F. Sohel, and F. Bousaid. A new representation of skeleton sequences for 3d action recognition. In *CVPR*, 2017.
- [16] D. P. Kingma and J. Ba. Adam: A method for stochastic optimization. *arXiv*, 2014.
- [17] T. N. Kipf and M. Welling. Semi-supervised classification with graph convolutional networks. *arXiv*, 2016.
- [18] I. Lee, D. Kim, S. Kang, and S. Lee. Ensemble deep learning for skeleton-based action recognition using temporal sliding lstm networks. In *ICCV*, 2017.
- [19] C. Li, Q. Zhong, D. Xie, and S. Pu. Skeleton-based action recognition with convolutional neural networks. In *ICMEW*, 2017.
- [20] W. Li, L. Wen, M.-C. Chang, S. Nam Lim, and S. Lyu. Adaptive rnn tree for large-scale human action recognition. In *ICCV*, 2017.
- [21] J. Liu, A. Shahroudy, D. Xu, A. C. Kot, and G. Wang. Skeleton-based action recognition using spatio-temporal lstm network with trust gates. *TPAMI*, 2018.
- [22] J. Liu, A. Shahroudy, D. Xu, and G. Wang. Spatio-temporal lstm with trust gates for 3d human action recognition. In *ECCV*, 2016.
- [23] J. Liu, G. Wang, L.-Y. Duan, K. Abdiyeva, and A. C. Kot. Skeleton-based human action recognition with global context-aware attention lstm networks. *TIP*, 2018.
- [24] J. Liu, G. Wang, P. Hu, L.-Y. Duan, and A. C. Kot. Global context-aware attention lstm networks for 3d action recognition. In *CVPR*, 2017.
- [25] M. Liu, H. Liu, and C. Chen. Enhanced skeleton visualization for view invariant human action recognition. *PR*, 2017.
- [26] J. Long, E. Shelhamer, and T. Darrell. Fully convolutional networks for semantic segmentation. In *CVPR*, 2015.
- [27] W. Luo, Y. Li, R. Urtasun, and R. Zemel. Understanding the effective receptive field in deep convolutional neural networks. In *NIPS*, 2016.
- [28] V. Nair and G. E. Hinton. Rectified linear units improve restricted boltzmann machines. In *ICML*, 2010.
- [29] A. v. d. Oord, S. Dieleman, H. Zen, K. Simonyan, O. Vinyals, A. Graves, N. Kalchbrenner, A. Senior, and K. Kavukcuoglu. Wavenet: A generative model for raw audio. *arXiv*, 2016.
- [30] R. Poppe. A survey on vision-based human action recognition. *Image and vision computing*, 2010.
- [31] A. Shahroudy, J. Liu, T.-T. Ng, and G. Wang. Ntu rgb+ d: A large scale dataset for 3d human activity analysis. In *CVPR*, 2016.
- [32] J. Shotton, A. Fitzgibbon, M. Cook, T. Sharp, M. Finocchio, R. Moore, A. Kipman, and A. Blake. Real-time human pose recognition in parts from single depth images. 2011.
- [33] C. Si, Y. Jing, W. Wang, L. Wang, and T. Tan. Skeleton-based action recognition with spatial reasoning and temporal stack learning. In *ECCV*, 2018.
- [34] S. Song, C. Lan, J. Xing, W. Zeng, and J. Liu. An end-to-end spatio-temporal attention model for human action recognition from skeleton data. In *AAAI*, 2017.
- [35] S. Song, C. Lan, J. Xing, W. Zeng, and J. Liu. Skeleton-indexed deep multi-modal feature learning for high performance human action recognition. In *ICME*, 2018.
- [36] K. Sun, B. Xiao, D. Liu, and J. Wang. Deep high-resolution representation learning for human pose estimation. In *CVPR*, 2019.
- [37] Y. Tang, Y. Tian, J. Lu, P. Li, and J. Zhou. Deep progressive reinforcement learning for skeleton-based action recognition. In *CVPR*, 2018.
- [38] A. Vaswani, N. Shazeer, N. Parmar, J. Uszkoreit, L. Jones, A. N. Gomez, Ł. Kaiser, and I. Polosukhin. Attention is all you need. In *NIPS*, 2017.
- [39] J. Wang, Z. Liu, Y. Wu, and J. Yuan. Mining actionlet ensemble for action recognition with depth cameras. In *CVPR*, 2012.
- [40] J. Wang, X. Nie, Y. Xia, Y. Wu, and S.-C. Zhu. Cross-view action modeling, learning and recognition. In *CVPR*, 2014.
- [41] P. Wang, W. Li, P. Ogunbona, J. Wan, and S. Escalera. Rgb-d-based human motion recognition with deep learning: A survey. *CVIU*, 2018.

- [42] X. Wang, R. Girshick, A. Gupta, and K. He. Non-local neural networks. In *CVPR*, 2018.
- [43] X. Wang and A. Gupta. Videos as space-time region graphs. In *ECCV*, 2018.
- [44] D. Weinland, R. Ronfard, and E. Boyer. A survey of vision-based methods for action representation, segmentation and recognition. *CVIU*, 2011.
- [45] J. Weng, M. Liu, X. Jiang, and J. Yuan. Deformable pose traversal convolution for 3d action and gesture recognition. In *ECCV*, 2018.
- [46] L. Xia, C.-C. Chen, and J. K. Aggarwal. View invariant human action recognition using histograms of 3d joints. In *CVPRW*, 2012.
- [47] W. Xiong, L. Wu, F. Alleva, J. Droppo, X. Huang, and A. Stolcke. The microsoft 2017 conversational speech recognition system. In *ICASSP*, 2018.
- [48] S. Yan, Y. Xiong, and D. Lin. Spatial temporal graph convolutional networks for skeleton-based action recognition. In *AAAI*, 2018.
- [49] G. Yu, Z. Liu, and J. Yuan. Discriminative orderlet mining for real-time recognition of human-object interaction. In *ACCV*, 2014.
- [50] K. Yun, J. Honorio, D. Chattopadhyay, T. L. Berg, and D. Samaras. Two-person interaction detection using body-pose features and multiple instance learning. In *CVPRW*, 2012.
- [51] P. Zhang, C. Lan, J. Xing, W. Zeng, J. Xue, and N. Zheng. View adaptive recurrent neural networks for high performance human action recognition from skeleton data. In *ICCV*, 2017.
- [52] P. Zhang, C. Lan, J. Xing, W. Zeng, J. Xue, and N. Zheng. View adaptive neural networks for high performance skeleton-based human action recognition. *TPAMI*, 2019.
- [53] P. Zhang, J. Xue, C. Lan, W. Zeng, Z. Gao, and N. Zheng. Adding attentiveness to the neurons in recurrent neural networks. In *ECCV*, 2018.
- [54] Z. Zhang. Microsoft kinect sensor and its effect. *IEEE multimedia*, 2012.
- [55] W. Zhu, C. Lan, J. Xing, W. Zeng, Y. Li, L. Shen, and X. Xie. Co-occurrence feature learning for skeleton based action recognition using regularized deep lstm networks. In *AAAI*, 2016.